p-type MWT: Integrated Cell and Module Technology

C.J.J. Tool, E.J. Kossen, I.J. Bennett

Energy research Center of the Netherlands
ECN Solar Energy, 1755 ZG Petten, The Netherlands

A major issue of concern in MWT solar cells is the increased leakage current at reversed bias voltage through the vias compared. At ECN we have been working on reducing this leakage current to levels comparable to H-pattern cells. In this study we present the results of this work.

We further show the benefit of a combined cell and module design for MWT solar cells. At the cell level, MWT production costs per wafer are comparable with H-pattern while the cell output increases. At the module level this design results in a further increase of the power output.

Introduction

The major goal of the PV industry nowadays is to lower the cost of solar photovoltaic electricity. This can be realized by either increasing the efficiency of the PV modules, or by reducing their production cost.

The vast majority of the PV-market still consists of (p-type) crystalline silicon (x-Si) PV. In x-Si modules, solar cells are usually interconnected in strings by tabs soldered to the front side of one cell and the rear side of the adjacent cell. Due to the limited width of the tabs, such interconnection leads to additional resistive losses. A promising option to reduce the resistive losses in the interconnection is by using an metal wrap through (MWT) concept, as shown in a recent review on this concept[1].

The MWT cell design places all the electrical contact points on the rear side of the cell. This is realized by bringing the emitter metallization via small holes (vias) through the wafer to the rear side of the cell. Compared to H-pattern processing, in the ECN approach the only additional cell process step is drilling the vias. This means that the ECN process can easily be installed as an update in most modern x-Si cell production lines.

To fully benefit from the MWT design, we developed interconnection based on conductive foil. In this process, cells are not interconnected by soldering tabs to the cells, but by a conductive back-sheet (Figure **1**). Cells are placed on the structured conductive back-sheet which connects the emitter contacts of one cell to the base contact of the adjacent cell and at the same time acts as the back- sheet of the module.
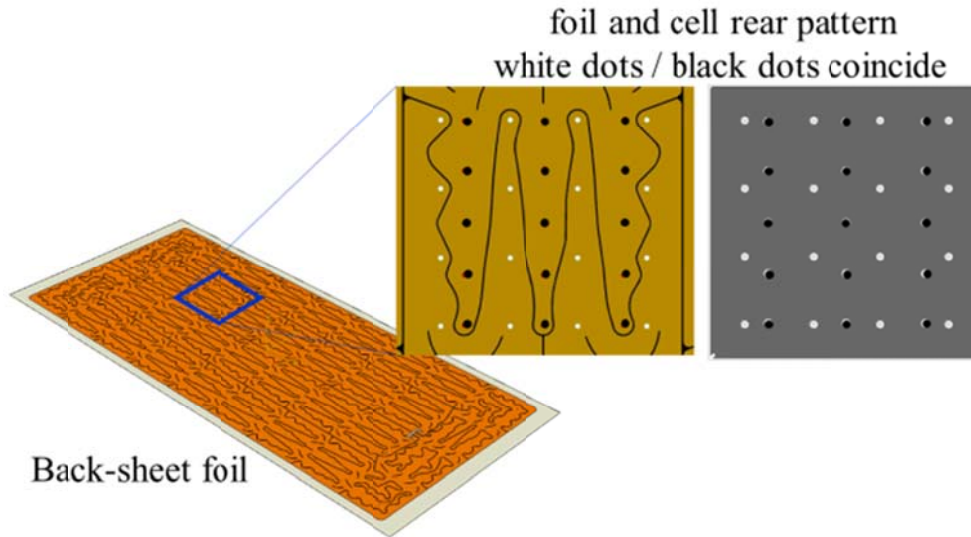
Figure 1: Integrated cell and module design. Dots of matching colors are connected using conductive adhesive.

In previous work we have observed an increase in the leakage current of ECN-MWT cells as compared to H-pattern cells[2]. This leakage current is related to the vias as illustrated in Figure 2. It is reported that ECN-MWT cells can tolerate higher leakage currents compared to H-pattern cells because the current is divided over more spots[3]. Also, modules manufactured from ECN-MWT cells bearing higher leakage current passed the IEC61730 hotspot tests easily[4]. However, hotspot test criteria might become more severe in the future, and industry also prefers lower leakage current.
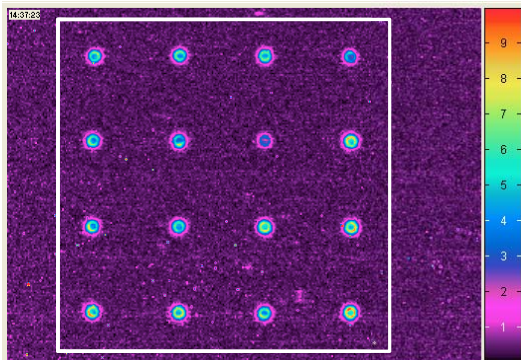
Figure 2: Vomolit[1] scan of MWT cell. White line indicates the position of the cell edge.

Therefore, in this work we focus on the reduction of the leakage current of MWT solar cells. We also show the benefits of the MWT design, both at cell and module level and the cost effectiveness of this integrated MWT concept.

---

[1] Vomolit: Voltage Modulated Lock In Thermography: while applying a (negative) voltage, the temperature of the cell is monitored by a sensitive IR camera. Temperature variations indicate ohmic warming of the cell[5].

Experimental Setup

Cell processing

The ECN-baseline process flow consist of an alkaline random pyramid texture etch followed by tube diffusion using $POCl_3$ as the phosphorous source. Wafers are loaded back-to-back in the $POCl_3$ tube to maximize the loading and minimize the processing costs. After diffusion a combined glass removal and pn-junction isolation using wet chemical single side etch is performed. The sheet resistance of the emitter is about 70 Ω.sq. A remote MW-PECVD system is used to deposit an ~80 nm thick single layer SiNx anti reflection coating. Finally the metallization is applied by screen printing and the contacts are co-fired in an IR heated belt furnace. A schematic overview of the process sequence is given in Table I.

The vias to guide the emitter contacts to the rear in the MWT approach are made using laser drilling. The position of the laser drilling step in the process flow can be varied, depending on the process being used in the industrial production line. Besides the vias and metallization patterns used, the H-pattern and MWT cells are processed using identical processes and process settings. This supports the introduction of MWT in existing Si-cell production lines.

Besides the standard process settings, we also included an MWT group with a more shallow emitter and a different front side metallization. This group is refered to as MWT$_{optimzoied}$ throughout this paper. Instead of the standard Circle MWT pattern we applied an H-lookalike pattern (Figure 3) for ease of modeling.

TABLE I. *H-pattern Process Flow*

Step	Process
1	random pyramid texture
2	$POCl_3$ emitter diffusion
3	PSG etch + Single Side Etch (SSE) parasitic junction removal
4	MW-PECVD SiN ARC deposition
5	contact printing (front and rear silver contacts + Al-BSF)
6	Co-firing metal contacts
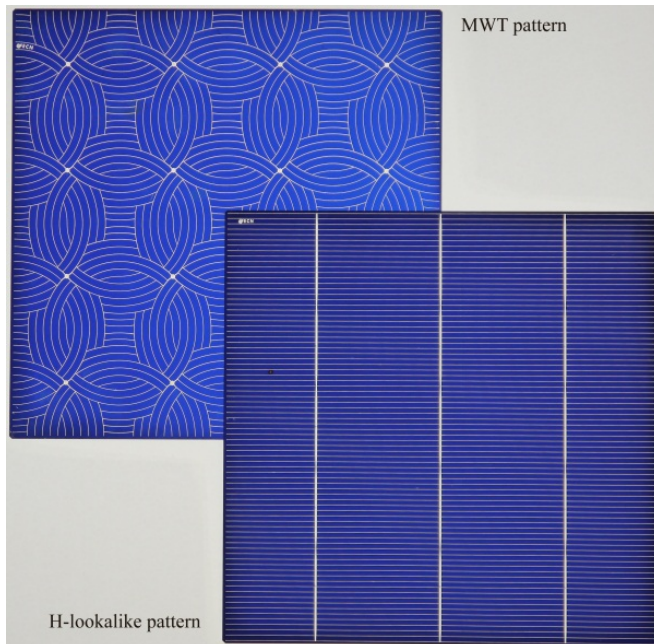
Figure 3: ECN's Circle MWT pattern (top left) and the H-lookalike MWT pattern (bottom right)

60 cells were selected to be mounted into a module. The H-pattern cells were interconnected using the normal industrial tabbing and soldering interconnection. The MWT cells were interconnected using a conductive rear side foil and conductive adhesive for the interconnection using the Eurotron pilot line at ECN.

Leakage Current tests

On cell level the variation in the leakage current at reversed bias (Irev) is higher for MWT cells as compared to H-pattern cells as is shown in Figure 4. We expect that the fluctuation is (partly) due to process variations.
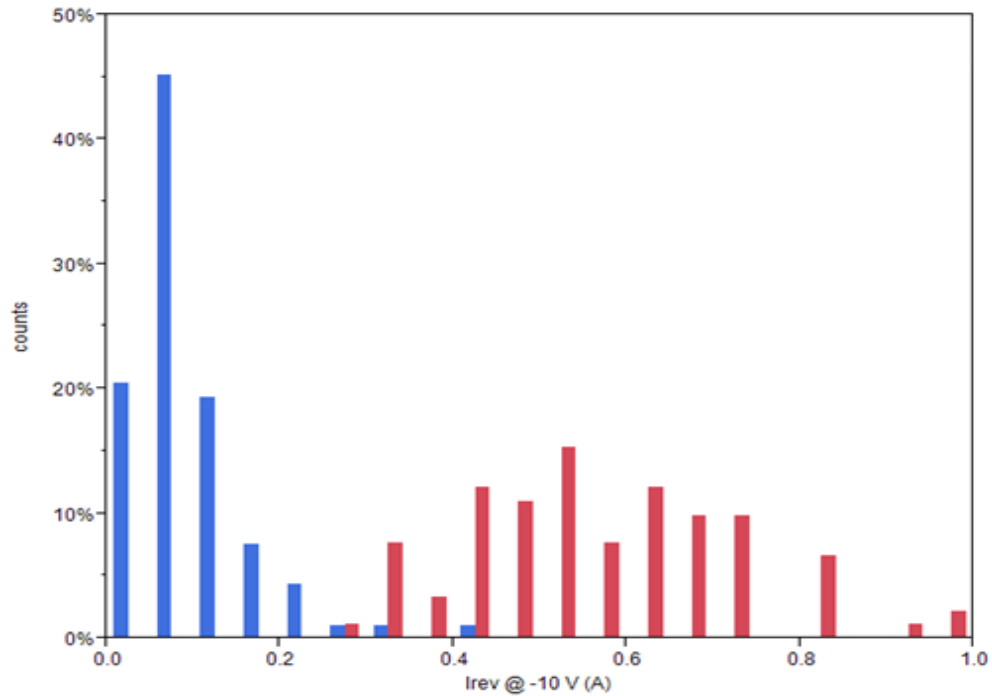
Figure 4: distribution of Irev measured at -10V. Blue is H-pattern, red is MWT

For comparing the effect of via paste on the Irev using only a limited number of samples, we designed a test structure which omits as much processing as possible. In using this test structure, the processing is limited to texture and rear side printing and firing. A comparison of the test structure to the real cell structure is given in Figure 5. In both structures no emitter is present between the Si-bulk and the via paste. Although this normally results in shunting, special precautions prevent this shunting behavior. ECN has a patent pending on this topic.

To measure the leakage current the test structure is placed on our in-house developed cell measurement chuck. An industrial Halm IV flash-tester is used to apply a voltage sweep of 0V to -13V on the test structure. During the sweep the leakage current is measured by the flash-tester.
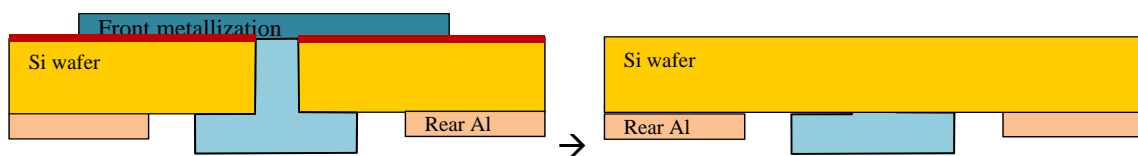
Figure 5: simplified test structure to evaluate Irev (right) compared to real cell structure (left).

Results and Discussions

Cell and module results

   3 groups of cells have been processed, each group about 100 wafers in size. Group 1 is the reference group. This group is processed using a standard H metallization pattern consisting of 2 busbars and 68 fingers. Group 2 is processed using the same process conditions as the H-pattern group. Only vias were laser drilled after SiN deposition and the metallization pattern is replaced by an MWT-pattern, the so called Circle pattern (see Figure 3). Group 3 is also an MWT group. The diffusion settings and metallization scheme are changed for this group as compared to group 2. Also the metallization design is changed into a H-lookalike pattern with 3 very small busbars and 80 fingers. Despite the use of the 3 busbars, the metallization area of group 3 is comparable to the metallization area of group 2. However, the use of the new paste in combination with screen parameters optimized for this paste resulted in a front side silver reduction of about 15% (see Table II.)

TABLE II. *Paste Consumption*

grp	pattern	Ag_{front} mg/cell	Ag_{rear} mg/cell	Al g/cell
1	H	175	40	2.0
2	MWT	170	42	2.0
3	MWT$_{improved}$	140	42	2.1

Table III. *IV characteristics H-pattern and 2 MWT scenario's*

grp	pattern	N	Isc A/cm^2	Uoc V	FF %	Eta %	$Irev_{@-10V}$ A
1	H	93	9.05	0.625	76.4	17.8	0.10
2	MWT	91	9.22	0.629	75.8	18.1	0.57
3	MWT$_{improved}$	124	9.26	0.632	77.4	18.6	0.37

   The increase in Isc for MWT compared to H-pattern is directly related to the lower front metallization area. The increase in Voc could be due to a different connection of the cell to the measurement system. However, also on the module level an increase in Voc is observed (see Table 4). Probably it results from less contact recombination because of the reduced metallization area[6]. Overall, on the cell level we observe an 0.3%$_{absolute}$ efficiency (1.6%$_{relative}$) efficiency increase for MWT when identical process settings are used (group 1 vs group 2).

   Table IV summarizes the IV characteristics of the modules. On module level the trends in Isc and Voc are comparable to the trends observed on cell level. As mentioned above, the smaller difference in Voc on the module level might originate from different contacting schemes for the H-pattern and MWT cells, while the contacting schemes for the modules are identical.
   Most remarkable is the small drop in FF for both MWT modules compared to the H-pattern module. For the MWT modules the drop in FF is only 1-1.5%, while the drop in FF for the H-pattern module is 5%. This is due to the use of a (module wide) contact foil instead of small busbars. The last column in Table IV shows the Cell to Module power change (CtM). This is a measure for the power difference between the bare cells as measured on the cell tester and the module as measured on the module flash tester It is

calculated from the sum of the power of the individual cells in the module, divided by the module power output. The high CtM value can also be maintained for the improved MWT processing. So the improvements on the cell level are maintained on the module level.

Table IV. *IV characteristics of the module*

grp	pattern	Isc	Voc	FF	P	CtM
		A	V	%	W	
1	H	8.83	37.69	71.0	236.3	0.910
2	MWT	8.92	37.83	75.0	253.0	0.957
3	MWT$_{improved}$	9.01	38.00	75.8	259.5	0.967

Leakage Current and Process Conditions

Firing conditions. The firing condition has a distinct influence on the leakage current. Increasing the belt speed or lowering the firing temperature both reduce the leakage current as indicated by the solid arrow in Figure 6. However, in order to maintain a good FF an increase in belt speed needs to be compensated by an increase in firing temperature and vice versa as indicated by the dashed arrow in Figure 6. This indicates that one can decrease the leakage current by adopting the firing condition, but then a more aggressive front side silver paste is needed to maintain a good FF.
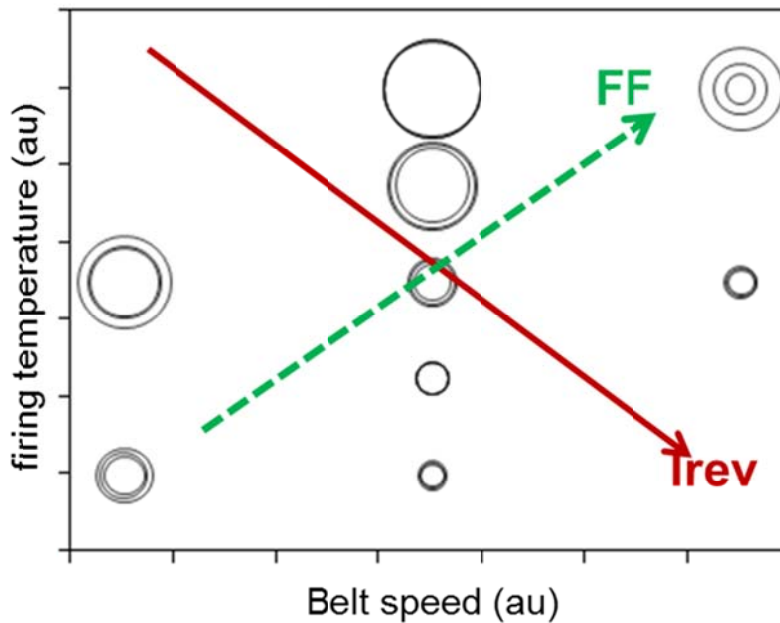
Figure 6: Impact of firing conditions (belt speed and firing temperature) on Irev. Size of the indicates the magnitude of the measured leakage current (0.3A – 5A)

Via paste tests. Instead of applying a new front side silver paste, we focused on the implementation of a new via paste. Several commercial paste manufacturers are developing dedicated via pastes. We tested in total 12 different via pastes from 3 suppliers. Most pastes behaved worse than the reference via paste, but 3 pastes gave excellent results on both Cz and mc-Si test structures (Table V).

TABLE V. leakage current measurements on mc-Si and Cz test structures

Paste	Irev @ -10 V (A)		Irev @ -12V (A)	
	mc-Si	Cz-Si	mc-Si	Cz-Si
Reference	0.35	0.46	0.46	0.71
A	0.05	0.17	0.07	0.21
B	0.22	0.21	0.27	0.25
C	0.17	0.06	0.21	0.07

We have observed for the reference via paste that the Irev value increased when we remeasured samples. To evaluate the stability of the via pastes we did repeating measurements on all pastes. The time between the measurements is about 1 second. As can be seen in Figure 7, all 3 new pastes behave much better than the reference paste. For the reference paste, the behavior on mc-Si and Cz-Si is comparable.
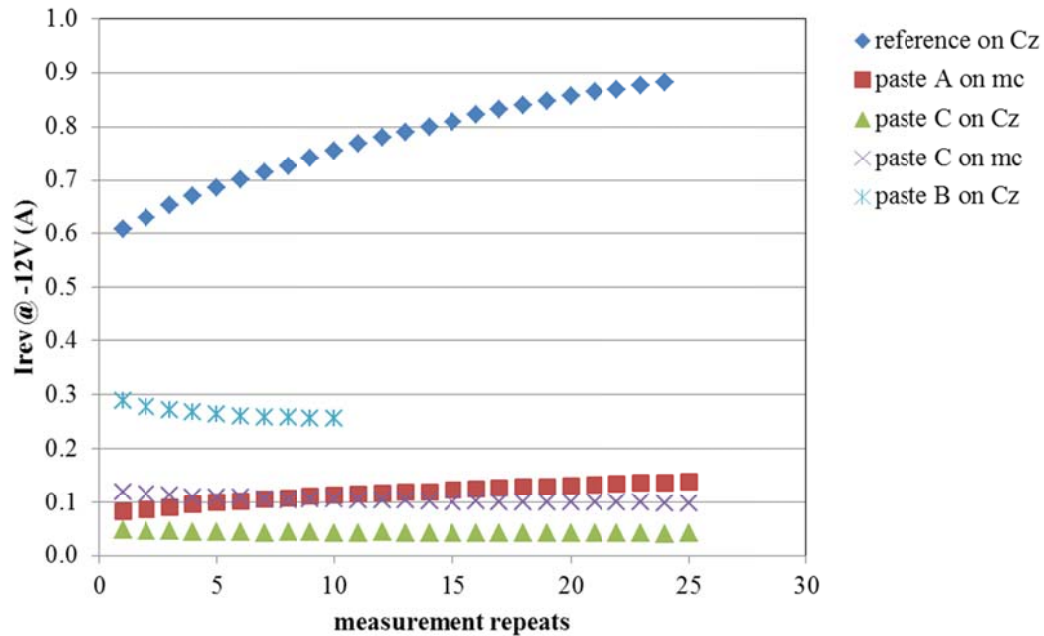
Figure 7: development of Irev @ -12V depending on the number of measurements

The first results on cell level confirm the good behavior of paste A. IV data for this paste are given in Table VI. Comparing these results with the IV characteristics obtained with the reference via paste in the MWT$_{improved}$ scenario (grp 3 in Table III) confirms the better Irev characteristics of via paste A. The other IV characteristics are slightly lower, but that might result from the use of a different batch of p-Cz wafers.

Cells were interconnected into 3 mini-modules of 2*2 cells each to confirm that conductive adhesive interconnection of the cells is still possible. As shown in Table VI the FF loss is slightly higher compared to the 60 cell modules fabricated with the reference via paste. However, the interconnection pattern is designed for full size modules and not for 2*2 mini-modules, while also the manufacturing of the mini-modules is done manually which can have resulted in a slightly higher series resistance.

TABLE VI. *IV characteristics of MWT$_{improved}$ scenario using via paste A.*

Device	N	Isc A/cm^2	Uoc V	FF %	Eta$_{cell}$ %	Irev$_{@-10V}$ A
Cell	18	9.23	0.631	76.8	18.4	0.11
2*2 module	3	9.07	2.52	74.4	17.4	

Cost Aspects of MWT cells & modules

In this chapter we will give a short discussion on the cost consequences of MWT. We will not discuss the overall cost structure, but limit ourselves to the cost differences between H-pattern and MWT.

Cell Costs

Compared to H-pattern cells processing, only the via drilling by laser is added for MWT cells. This laser will add about 250-350 k€to the investment for a production line. This higher investment is paid off by the lower silver consumption of the MWT cells. Therefore, the manufacturing costs of H-pattern and MWT cells can be considered comparable. Because of the higher efficiency of the MWT cells, the cost/Wp is lower for MWT.

Module Costs

The differences in cost between H-pattern and MWT modules are related mostly to the difference in module materials[7]. In the MWT module, the conductive back-sheet and conductive adhesive replaces the back-sheet, tabbing and bussing used in an H-pattern module. The use of mechanical patterning for the backsheet foil resulted in a substantial cost reduction for the MWT module.

Extensive calculations by Eurotron show that the MWT module is about 6% cheaper in €/Wp compared to an H-pattern module with the same number of cells[7].

System Cost

The MWT-module can be made smaller than a comparable H-pattern module as the cells can be placed closer together and the bussing is integrated in the conductive back-sheet. Therefore the power output per unit area is even larger than the difference in generated power. As part of the balance of system (BoS) cost scale with area, the smaller MWT-module will result in additional savings at the system level. Furthermore, MWT modules have been shown to generate a larger annual energy output, particularly at high irradiance[8], further reducing the €/kWh costs.

Conclusion

In this work we showed that we can reduce the leakage current of MWT cells to values comparable to H-pattern cells. Although the first results indicate a small drop in cell efficiency we expect that we can recover this by further optimizing the paste.

References

1. E. Lohmüller, M. Hendrichs, B. Thaidigsmann, U. Eitner, F. Clement, A. Wolf, D. Biro, R. Preu, *Photovoltaics International, 17, 61-71,* (August 2012)
2. C.J.J. Tool, E.J. Kossen, I.J. Bennet, M.J.H. Kloos, W. Eerenstein, *22nd PVSEC, Hangzhou, (2012)*
3. M.J. Jansen, L.A.G. Okel, R.A. van der Schilden, I.G. Romijn, B.J. Geerligs, B.B. van Aken, *22nd PVSEC, Hangzhou, (2012)*
4. M. Späth, *personal communication*
5. M. Kaes, S. Seren, T. Pernau, G. Hahn, *Progr. Photovolt: Res. Appl. 12, 355-363 (2004)*
6. R. Hoenig, A. Kalio, J. Sigwarth, F. Clement, M. Glatthaar, J. Wilde, D. Biro, *Sol. Energy Mater. Soll. Cells, 106, 7-10,* (2012)
7. B. Verschoor & J. Bakker, *4th Workshop on MWT solar cell and module technology, Amsterdam, (2012)*
8. N.J.J. Dekker, M.J. Jansen, I.J. Bennett, W. Eerenstein, *Proceedings 27th EUPVSEC, Frankfurt,* (2012)